Journal of Molecular Structure 1246 (2021) 131152

Contents lists available at ScienceDirect

Journal of Molecular Structure

journal homepage: www.elsevier.com/locate/molstr

Design, synthesis, and evaluation of some novel biphenyl imidazole derivatives for the treatment of Alzheimer's disease

Salunke Prashant Ramrao, Akash Verma, Digambar Kumar Waiker, Prabhash Nath Tripathi, Sushant Kumar Shrivastava*

Pharmaceutical Chemistry Research Laboratory, Department of Pharmaceutical Engineering & Technology, Indian Institute of Technology (Banaras Hindu University), Varanasi, India

ARTICLE INFO

Article history:
Received 21 March 2021
Revised 17 July 2021
Accepted 19 July 2021
Available online 21 July 2021

Keywords:
Alzheimer's disease
Aβ aggregation
β-Secretase-1 (BACE-1)
Acetylcholinesterase (AChE)
Multi-functional agents
Bio-isosteric

ABSTRACT

The multi-targeted organized strategy provides effectual and significant results to cure progressive neurodegenerative diseases like AD. Treatment for this awful disease is in infancy till now. A series of novel 4, 5-diphenyl-1*H*-imidazole linked piperazine hybrids (**6a-g** and **7a-g**) were synthesized by utilizing the concept of bio-isosteric replacement and hybrid pharmacophore approaches. The targeted compounds were identified by spectroscopic techniques and assessed for *in vitro* cholinesterase, BACE-1 inhibition, propidium iodide displacement, and Aβ disaggregation activities. Within the targeted inhibitors, **6f** exhibited the most significant and inhibitory capacity against eeAChE (IC_{50} = 0.416 ± 0.018 μM), eqBChE (IC_{50} = 0.474 ± 0.054 μM), and BACE-1 (IC_{50} = 0.392 ± 0.021 μM) targets. Propidium iodide displacement showed that compound **6f** could be effectively linked with AChE's PAS (10 μM = 29.09 %, 50 μM = 41.43%). It showed inhibitory potential against both self (21.28 to 30.85%) and AChE-induced (25.70 to 51.07%) Aβ aggregation in thioflavin T assay. Moreover, the most active compound **6f** was evaluated by performing *in vivo* behavioural studies with the help of the scopolamine-induced Y-maze model. The *in vitro* and *in vivo* in collaboration with *in silico* molecular docking and molecular dynamics simulation leads to ascertain the active site interaction of compound **6f** with AChE and BACE-1.

Abbreviations

AD	Alzheimer's Disease
Aβ	Amyloid-beta
NMDAR	N-methyl D-aspartate receptor
CREB	cAMP response element-binding protein
ChE	Cholinesterase
eeAChE	Electrical eel Acetylcholinesterase
eqBChE	Equine serum Butrylcholinesterase
BACE-1	Beta-site amyloid precursor protein cleaving enzyme-1
APP	Amyloid precursor protein
AChEIs	Acetylcholinesterase inhibitors
MDLs	Multitarget-directed ligands
CAS	Catalytic active site
PAS	Peripheral anionic site
PI	Propidium iodide
R_f	Retention factor
MD	Molecular dynamics
RMSD	Root mean square deviations
RMSF	Root mean square fluctuations
ACN	Acetonitrile
K_2CO_3	Potassium carbonate
DTNB	5,5-dithio-bis-(2-nitrobenzoic acid)
ATCI	Acetylthiocholine iodide
BTCI	Butyrylthiocholine iodide.

1. Introduction

Alzheimer's disease (AD) is considered a complex progressive neurodegenerative disease, and it is identified by the gradual decline of cholinergic neuronal cells and accumulation of amyloid-beta (Aβ) proteins in the brain area like the cortex and hippocampus. The progression starts with short-term memory impairment that gradually progresses to complete loss of cognitive function, weak performance, loss of logical thoughts, and ultimately death [1]. Due to its complex nature, it may lead to the cause of both emotional as well as financial load. One of its atrocious and critical aspects is the deprivation of cognitive capabilities that recently calculate for more than 50 million cases globally and it is expected that this number will cross more than triple by 2050 [2]. The preponderance of 10 – 30% and incidence of 1 – 3 % of the AD belongs to the population having age more than 65 years

* Corresponding author.
E-mail address: skshrivastava.phe@itbhu.ac.in (S.K. Shrivastava).

https://doi.org/10.1016/j.molstruc.2021.131152
0022-2860/

which represents the inexorable effect of aging [3]. AD is correlated with various pathophysiological hallmarks like declination in acetylcholine (ACh) levels [4], assembling of Aβ [5], N-methyl-D-aspartate receptor (NMDAR) hyper-activation [6], tau protein hyperphosphorylation and assembling of neurofibrillary tangles [7], inflammation of CNS and neuronal cells [8], gene transcription by CREB (cAMP response element-binding protein) signaling and oxidative stress [9]. Cholinesterase (ChE) is considered as a serine hydrolytic enzyme including acetylcholinesterase (AChE) and butyrylcholinesterase (BChE) that help in the progression of AD by rapidly hydrolyzing the ACh that results in the termination of signaling at the cholinergic synaptic cleft. However, specific cholinesterase inhibition by currently available drugs provides only symptomatic relief [10]. AChE is also involved in the formation of Aβ aggregates in Alzheimer's disease. [11]. β-secretase-1 is also considered as a beta-site amyloid precursor protein cleaving enzyme-1 (BACE-1) that disintegrates amyloid precursor protein (APP) and formed amyloid peptides which are further accompanied by a combination of oligomeric reactions and lead to the formation of oligomers, fibrils, and plaques [12]. All these reactions integrate and perform an important role in the aggregation of Aβ and interrupt the various cellular communications, inflammatory responses, neuronal abnormalities, behavior alterations, etc. [1314].

Recently, no remedies are present for the cure of the disease. FDA-approved medications such as acetylcholinesterase inhibitors (AChEIs) (donepezil, rivastigmine, galantamine) and NMDA-inhibitor (memantine) have been used in recent treatment plans [15]. Moreover, treatment for the awful ailment in the development phase till now. Recent findings are directed towards a highly promising strategy that includes the evolution of multi-targeted and multi-functional pharmacophore to cure this multifaceted disorder. Among several drug discovery strategies, the multitarget-directed ligands (MDLs) strategy is the most promising recent approach as it involves targeting multiple enzymes responsible for AD at the same time by a single compound. Hence, this MDLs approach provides not only symptomatic relief but also proves appreciable in the mitigation of the disease progression [16].

To design and develop the multi-functional molecular hybrid, a literature survey of some recently reported compounds was utilized. Literature study showed that advanced series with different hetero-aromatic rings such as imidazole, benzimidazole, thiazole, indanone, coumarin, piperidine derivatives showed promising inhibitory activity against AChE and BACE-1 inhibition [17–23]. Based on the literature survey, diaryl 1, 2, 4-triazine scaffold was utilized due to its interaction capabilities and better inhibition potential against several enzymes especially cholinesterase enzymes [24–27]. Among diaryl 1, 2, 4-triazine scaffolds, 5, 6-biaryl of (**1**) proved to be an appropriate moiety that gained the capability in anchoring the peripheral anionic region of AChE by creating a hydrophobic environment [28]. Replacement of 1, 2, 4-triazine group with thiazole moiety and linking with benzyl piperidine not only acquired a significant improvement in the binding parameters but also (**2**) improve the inhibitory activity profile [29]. Further replacement of sulfur (S) of thiazole by nitrogen (N) (**3**) seeks the new diaryl-imidazole scaffold with improved memory and cognitive abilities, as well as a reduction in progressive neurodegeneration. By employing the above-mentioned approaches, 4, 5-diphenyl-1*H*-imidazole was developed as a core moiety and bounded with other pharmacophoric characteristics [18]. FDA-approved drug containing benzyl piperidine moiety named donepezil used to treat dementia is conformed into the catalytic active site (CAS) of AChE [30]. Bioisosteric replacement of piperidine with piperazine proved a lower affinity for AChE but improved the inotropic impact with significant neuro-protective activity [31].

Based on these prior studies and facts, a classic bio-isosteric bivalent approach for the design of new hybrid molecules was introduced and it was planned to connect the 4, 5- diphenyl-1*H*-imidazole ring and substituted piperazine with different lengths of alkyl linkers to seek a novel 4, 5-diphenyl-1*H*-imidazole linked piperazine hybrids. It was considered that the 4, 5 diphenyl-1*H*-imidazole core of the constructed hybrids would bind with the peripheral anionic site (PAS) of AChE and the piperazine fragment would interact with the CAS region of AChE. Thus, the designed 4, 5-diphenyl-1*H*-imidazole linked piperazine hybrids could demonstrate multi-target-directed AD management potential (Fig. 1).

The proposed compounds were synthesized, identified, and biologically assessed against ChE and BACE-1 targets. The binding ability of active compounds with PAS was achieved by propidium iodide (PI) displacement assay. For their anti-Aβ activity, active compounds were also evaluated in self and AChE-induced experiments with the help of thioflavin T assay. Most promising compounds were evaluated for their capability to cognitive impairment in scopolamine-induced AD rat models. Molecular docking studies were also performed in the most active compound.

2. Results anddiscussion

2.1. Chemistry and physicochemical characterization

The target compounds **(6a-g** and **7a-g)** were prepared according to reactions involved in the Scheme 1. Initially, compound **1** was reacted with bromo chloro substituted alkanes along with the addition of dry potassium carbonate (K_2CO_3) and acetonitrile (ACN) gave **2** and **3** intermediates [32]. In ^{1}H NMR spectra, compound **1** having singlet of (-O**H**) proton peak was disappeared and a triplet signal of (-O-C**H$_2$**) between was appeared in between 4.36 – 4.17 ppm. Also, ^{13}C NMR spectra exhibited the characteristics signal of (-O-**C**H$_2$) and (-**C**H$_2$-Cl) at 67.96 – 64.62 ppm and 31.96 – 28.48 ppm, respectively, confirmed the formation of **2** and **3** intermediates. The obtained intermediates were further refluxed with benzoin in presence of ammonium acetate, cerric ammonium nitrate, and ethanol:water (1:1, v/v) to yield key intermediates **4** and **5** [33]. In ^{1}H NMR spectra, the singlet peak of (-C**H**) proton of benzaldehyde was disappeared and the appearance of singlet peak of (-N**H**) proton of imidazole ring at 12.66 – 12.53 ppm and appearance of multiplet of 10 biphenyl protons at 7.77 – 7.15 ppm confirmed the formation of **4** and **5** intermediates. Also in ^{13}C NMR spectra of **4** and **5** intermediates, the disappearance of carbonyl (**C**=O) peak of benzaldehyde and appearance of resonance signal for (N=**C**-NH) sp^2 hybrid carbon of imidazole ring in the range of 158.54 – 153.23 ppm. By refluxing the **4** and **5** intermediates with different substituted piperazine in the presence of potassium iodide, anhydrous potassium carbonate, and acetonitrile, the final compounds (**6a-g** and **7a-g**) were obtained. The Dragendroff reagent was used to recognize the compounds that were obtained [34]. The absence of singlet peak of (-N**H**) of piperazine and presence of the triplet signal of (-N-C**H$_2$**) in a range of 3.11 – 2.62 ppm, also the appearance of characteristic (-N-**C**H$_2$) peak at 57.20 – 53.00 ppm in ^{13}C NMR spectra confirmed the formation of final compounds (**6a-g** and **7a-g**). In ^{1}H NMR spectra, the compounds **6b** and **7b** having 2-pyridyl moiety substituted on piperazine exhibited a resonance signal of an aromatic proton between 8.18 – 6.58 ppm. Methoxy group of substituted piperazine of compound **6c** and **7c** showed characteristic singlet peak of (C**H$_2$**-O-) at 3.66–3.59 ppm. Methylene protons (N-C**H$_2$**-C$_6$H$_5$) of benzyl piperazine of compounds **6f** and **7f** displayed a singlet peak at 3.56 - 3.54 ppm. Compounds **6g** and **7g** having benzhydryl methyl (-C**H**) group of substituted piperazine gives a diagnostic singlet peak at 5.18 – 5.15 ppm. In ^{13}C NMR spectra, compounds **6c** and **7c** with 4-methoxyphenyl substitution on piperazine exhibits NMR signal of

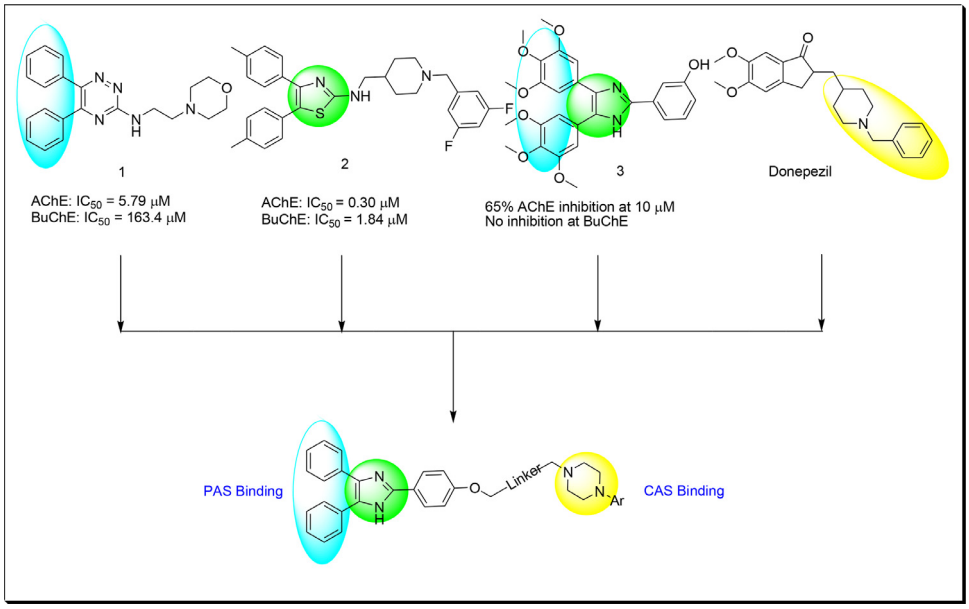

Fig. 1. Designing strategy of targeted compounds.

Table 1
The results of eeAChE, eqBChE, and BACE-1 inhibition assay.

Comp. Code	n	Ar	IC_{50} (μM) ± SEM[a] eeAChE	eqBChE	BACE-1	SI ratio[b]
6a	2	-C_6H_5	3.056 ± 0.442	> 10	6.242 ± 0.530	-
6b	2	-C_5H_4N	1.132 ± 0.067	3.463 ± 0.013	4.785 ± 0.371	3.05
6c	2	4-$OCH_3C_6H_5$-	0.751 ± 0.043	1.217 ± 0.374	1.485 ± 0.095	1.62
6d	2	4-$NO_2C_6H_5$-	1.153 ± 0.179	3.357 ± 0.054	1.685 ± 0.012	2.91
6e	2	4-FC_6H_5-	0.917 ± 0.271	2.498 ± 0.375	1.342 ± 0.078	2.72
6f	2	-CH_2-C_6H_5	0.416 ± 0.018	0.474 ± 0.054	0.392 ± 0.021	1.13
6g	2	-$CH(C_6H_5)_2$	>10	>10	>10	-
7a	3	-C_6H_5	1.549 ± 0.023	1.836 ± 0.054	3.811 ± 0.339	1.18
7b	3	-C_5H_4N	1.435 ± 0.164	1.922 ± 0.121	5.622 ± 0.346	1.33
7c	3	4-$OCH_3C_6H_5$-	0.467 ± 0.021	0.826 ± 0.038	0.922 ± 0.103	1.76
7d	3	4-$NO_2C_6H_5$-	1.409 ± 0.054	4.481 ± 0.376	2.037 ± 0.249	3.18
7e	3	4-FC_6H_5-	1.313 ± 0.022	3.032 ± 0.081	1.934 ± 0.245	2.30
7f	3	-CH_2-C_6H_5	0.697 ± 0.047	2.354 ± 0.753	1.792 ± 0.287	3.37
7g	3	-$CH(C_6H_5)_2$	>10	>10	>10	-
Donepezil	-	-	0.033 ± 0.01	1.4 ± 0.06	0.24 ± 0.03	42.4

[a] -Results are expressed as the mean IC_{50} ± SEM (n = 3);
[b] -SI (selectivity index) = IC_{50} of BChE/IC_{50} of AChE;

(**C**H_3-O-) and carbon attached to it between 54.63 – 54.19 ppm and 145.88 – 145.21 ppm, respectively. Compounds **6f** and **7f** having methyl (-**C**H_2) group of benzyl substituted piperazine showed characteristics resonance signal at 63.72 – 62.82 ppm. The synthesized compounds **6g** and **7g** bearing benzhydryl substitution on piperazine exhibited distinctive NMR signal for biphenyl methyl (-**C**H) approximately between 77.67 – 77.04 ppm.

2.2. In vitro *evaluation*

2.2.1. *Cholinesterase inhibition assay (eeAChE and eqBChE)*

The targeted compounds **6a-f** and **7a-f** were evaluated by the Ellman technique using donepezil as beneficial reference norms for their inhibitory capacity against eeAChE and eqBChE. The ChE enzymes inhibition activity of various targeted compounds were examined with regards to the variation of alkyl linkers (n = 2, 3) as well as substituent linked with the endpoint of piperazine scaffold (Table 1).

Variation of alkyl chain linker

Alkyl linkers (n = 2, 3) constructed a bridge between 4, 5 diphenyl-1*H*-imidazole and substituted phenyl piperazine scaffold. Targeted compounds were analyzed for their ChE activity profile. The ability of these compounds to prevent AChE was influenced by the length of the bridge and the freedom of rotation around the two-atom connecting structure [35,36]. Hence, it was found that targeted compounds exhibited 2 carbon chain linkers provided better output.

The compounds (**6g, 7g**) possessing benzhydryl piperazine moiety at the endpoint did not provide any appropriate inhibition potential due to enhanced hydrophobicity lowers the binding potential of targeted compounds to the AChE region [37].

Variation of terminal piperazine functionalities

The results exhibited moderate to excellent eeAChE inhibition in the concentration range of micromolar to sub-micromolar except for the compounds **6g, 7g** (IC_{50} > 10 μM). The eeAChE inhibition was checked by both the electron-donating (methoxy, **6c**) and electron-withdrawing (nitro, **6d**; and fluoro, **6e**) groups at the fourth position of phenyl piperazine ring (**6c**, IC_{50}: 0.751 ± 0.043 μM; **6d**, IC_{50}: 1.153 ± 0.179 μM; **6e**, IC_{50}: 0.917 ± 0.271 μM) and expressed that compound **6c** with a 4-methoxyphenyl substituent on piperazine showed stronger inhibition of eeAChE compared to **6d** and **6e** compounds. The increase in eeAChE inhibitory

capacity could be due to the O-CH_3 group with non-polar features that interacted with eeAChE hydrophobic pocket [3]. Comparing compounds with distinct electron-withdrawing substituents, fluoro substituted compound **6e** showed a mildly good inhibitory ability against eeAChE compared to nitro substituted compound **6d**. An improved inhibitory activity might be due to the elevated fluorine atom electronegativity that influences the molecule's lipophilicity. The compound having a 2-pyridyl substituent on piperazine (**6b**) exhibited reduced inhibition of eeAChE (IC_{50}: 1.132 ± 0.067 μM) compared to **6c, 6e**, and **6f** compounds. The compounds (**6g** and **7g**) comprising benzhydryl piperazine moiety at the endpoint and having various linkers showed no compelling results. It was already disclosed that elevated hydrophobicity blocks the binding of the compounds at the AChE's region [37]. Among all the evaluated compounds, compound **6f** containing two carbon connected to the phenyl piperazine end group showed significant inhibition of eeAChE (IC_{50}: 0.416 ± 0.018 μM). Due to the benzyl group which involved showed better interaction with AChE's CAS residues, Compound **6f** eeAChE inhibitory potential was also compared to that of donepezil (IC_{50}: 0.033 ± 0.01 μM). All the targeted compounds for their eqBChE inhibitory activity were further evaluated. Compounds **6c** and **6f** demonstrated excellent eqBChE inhibitory activity (**6c**, IC_{50}: 1.217 ± 0.374 μM; **6f**, IC_{50}: 0.474 ± 0.054 μM). Compounds **6b, 6d** and **6e** showed moderate inhibitory potential against eqBChE with an IC_{50} value ranging from 2.498 ± 0.375 µM to 3.463 ± 0.013 μM and compounds **6a, 6g**, and **7g** did not show important eqBChE inhibitory activity (IC_{50} > 10 μM). The wider eqBChE gorge than eeAChE, which results from the replacement of two aromatic amino acids by lower aliphatic amino acids, may be the cause [38].

2.2.2. BACE-1 inhibition assay

Using the FRET-based BACE-1 fluorescence assay kit, all targeted compounds were analyzed for inhibitory activity against BACE-1 (Table 1). The electron-donating (methoxy, **6c**) and electron-withdrawing (nitro, **6d**; and fluoro, **6e**) groups at the para position of phenyl piperazine fragment showed moderate inhibitory activity against BACE-1 with an IC_{50} value ranging from 1.342 ± 0.078 to 1.685 ± 0.012 μM. Compounds **6a, 6b,** and **6g** showed no important inhibitory activity of BACE-1.

Compound **6f** with two carbon atoms connected to the terminal group of benzyl piperazine showed a powerful inhibition of BACE-1 (IC_{50}: 0.392 ± 0.021 μM). Compound **6f** was chosen for further screening with promising inhibitory potential for both the targeted enzymes (eeAChE and BACE-1).

2.2.3. Propidium iodide displacement assay

Propidium iodide assay was used to check propidium iodide displacement from the enzyme complex of propidium iodide-AChE [39]. Propidium iodide is a recognized AChE complex that binds particularly at PAS and increases the intensity of fluorescence up to several fold [40]. Binding compounds at AChE's PAS results in decreased fluorescence intensity with propidium iodide displacement. Compound **6f** showed a greater propidium iodide displacement (10 μM = 29.09%, 50 μM = 41.43%) relative to donepezil (10 μM = 24.86%, 50 μM = 36.31%). Compounds **6c** exhibited relatively equal propidium iodide displacement (10 μM = 24.12%, 50 μM = 37.20 %) as compared to donepezil. Compounds **6b** and **6e** seemed to be less able to displace the propidium iodide of PAS-AChE (**6b** 10 µM = 15.03%, 50 μM = 21.77%; **6e** 10 μM = 20.15%, 50 μM = 24.29%). The results showed that compound **6f** could be effectively linked to AChE's PAS site (Fig. 2).

All the results are reported as the mean ± SEM (n = 3); Propidium iodide displacement assay was performed on AChE to assess the ability of compounds to displace propidium with reference to donepezil at 10 and 50 μM.

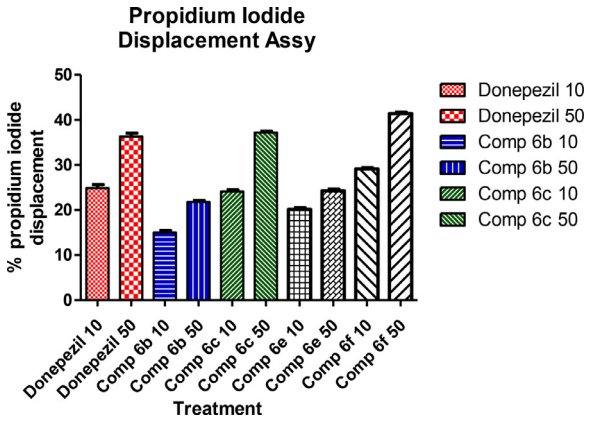

Fig. 2. Result of Propidium iodide displacement assay.

2.2.4. Aβ inhibition- thioflavin T assay

The AChE has also been shown to be indulged in promoting Aβ aggregation by interacting particularly with PAS [41]. AChEIs linked to the PAS can not only inhibit AChE, but also help prevent Aβ development and deposition. Therefore, a fluorometric assay based on thioflavin T was conducted on compound **6f** to determine their binding to the PAS region which could be useful in the prevention of Aβ aggregation. The experiment was performed at three distinct Aβ: inhibitor ratios (10:5, 10:10, and 10:20 µM). The percentage of Aβ aggregation inhibition was recorded (Fig. 3A and B). The inhibitor (**6f**) exhibited greater anti-aggregator property in self (21.28 to 30.85%) and AChE-induced (25.70 to 51.07%) studies compared with donepezil (Self-induced: 14.59 to 21.17%; AChE-induced: 19.72 to 33.05%). The findings verified these inhibitors' PAS-AChE binding capacity.

2.3. In vivo *evaluation*

2.3.1. Scopolamine-induced amnesia models for testing cognition enhancement in rats

Compound **6f** was evaluated for cognition and memory by performing behavioral studies with the help of the scopolamine-induced Y-maze model. To persuade cognitive impairment, a gold standard drug, scopolamine was administered [42]. Test compound in a dose of 2.5, 5, and 10 mg/kg, p.o., was given daily to healthy male Wistar rats. On the seventh day of the study, a Y-maze experiment was performed to determine the effect of compound **6f**, and spontaneous alternations, a measure of spatial working memory, were estimated. The proportion of spontaneous alternations was significantly lower (Fig. 4A, $p < 0.001$) in the scopolamine group of animals relative to the control group, indicating induction of memory and learning disability. In comparison with scopolamine, Donepezil (5 mg/kg) showed considerably enhanced spontaneous alternations (Fig. 4A, $p < 0.001$). As compared to donepezil, compound 6f (10 mg/kg) showed a statistically non-significant difference in the percentage of spontaneous alterations (Fig. 4A, $p < 0.001$). The complete arm in all groups stayed unchanged inferred that scopolamine did not interfere with locomotor capability in rats. The general findings of scopolamine-induced models supported compound **6f's** ability to improve spatial and immediate memory.

2.4. Computational studies

2.4.1. In silico *molecular docking studies*

Compound **6f** was monitored for its binding affinity and binding pattern on active site residues of AChE (PDB Code: 4EY7), BChE (PDB Code: 4TPK), and BACE-1 (PDB Code: 2ZJM) by conducting

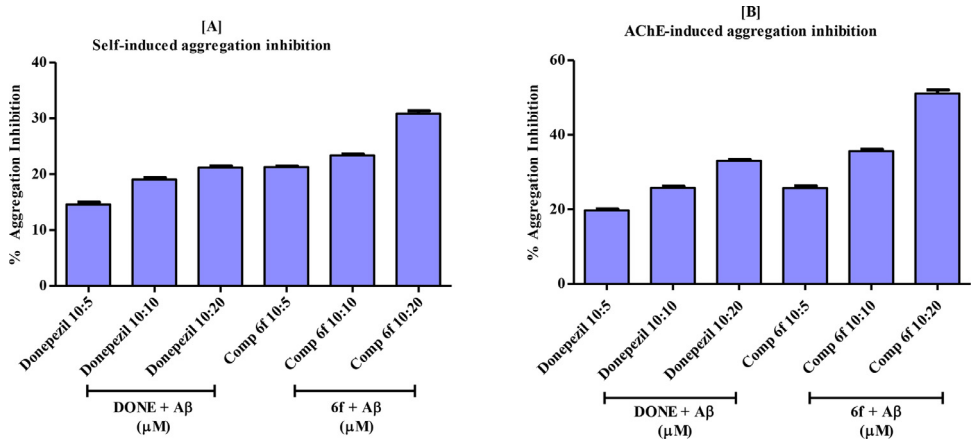

Fig. 3. [A] Self-induced and; [B] AChE-induced Aβ aggregation inhibition experiment. Results are expressed as the mean ± SEM of three independent experiments.

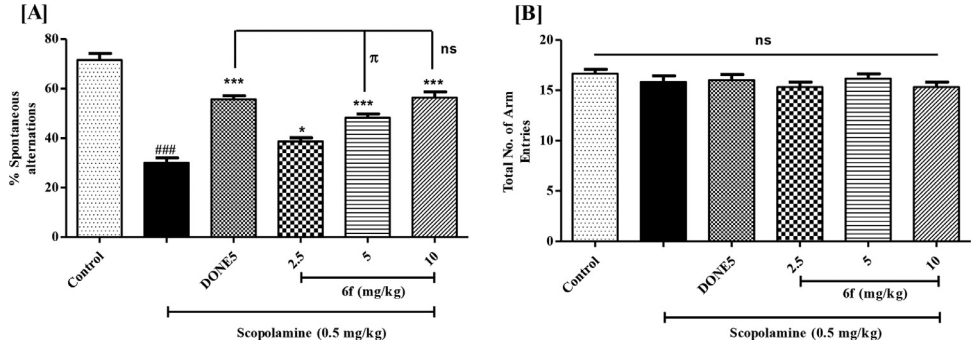

Fig. 4. Effect of compound 6f on scopolamine-induced cognitive deficit in the Y-maze test. [A] Spontaneous alteration (%) and; [B] Total arm entries in the Y-maze experiment. All result are showed as the mean ± SEM (n = 6). ###p < 0.0001 versus control; ***p < versus scopolamine; πp < 0.05, ns = non-significant versus DONE5 (donepezil 5 mg/kg).

molecular docking studies using Schrodinger Maestro's Glide module 2018–1. On AChE's active site, compound **6f** and donepezil showed the docked scores -15.566 and -15 kcal/mole, respectively. According to the docking study, the compound **6f** was found to bind likely with AChE's CAS and PAS region. Benzyl piperazine portion of the compound **6f** exhibited polar interactions with AChE's (CAS) residues His447 and Ser203. At the AChE's (PAS), compound **6f** interacted with Tyr72, Tyr124, Tyr341 residues through hydrophobic interactions, with Trp286 residue through hydrophobic as well as π-π stacking interactions and with Asp74 residue through charged interaction. Compound **6f's** benzyl piperazine portion developed hydrophobic, π-π, and π-cation interactions with the Trp86 residue of AChE's anionic location.

At the same site, it also formed hydrophobic and charged interactions with Phe338 and Glu202 residues, respectively. The linker part of compound **6f** showed hydrophobic interactions with Phe295 and Phe297 residues in the acyl binding pocket of AChE. Benzyl substituent of compound **6f** binds with Gly120 and Gly121 residues of the oxyanion site of AChE via glycine interactions (Table 2). Other residues of AChE also showed interactions with compound **6f**, like Tyr133, Leu76, Val294, Tyr337, and Ile451 residues interacted via hydrophobic interactions, Thr75, and His287 residues via polar interactions, and Gly448 residue via glycine interaction (Fig. 5).

Compound **6f** also showed their strong binding affection and binding pattern with the BChE active site. The piperazine moiety of compound **6f** displayed polar interactions with Ser198 and His438 residues of BChE's CAS. Also, the His438 residue displayed hydrogen bonding with compound **6f**. Asp70 (charged interaction) and Tyr332 (π-π stacking and hydrophobic interactions) residues of

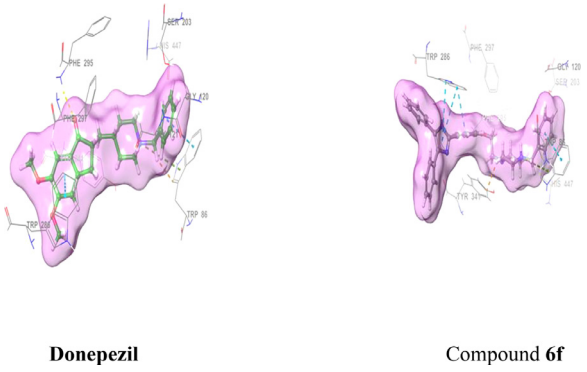

Fig. 5. Molecular docking of donepezil and compound 6f in the gorge of AChE enzyme. 3D pictorial image representing the interaction of donepezil and compound 6f in ligand binding surface (magenta color) with AChE active site.

PAS of BChE interacted with compound **6f**. At the anionic site of hBChE, Trp82 (hydrophobic and π-cation interactions) and Glh197 (charged interaction) residues showed binding with benzyl piperazine moiety of compound **6f**. Ala328 residue also showed hydrophobic interaction with compound **6f** at this site. Compound **6f** interacted with Gly116 residue in the oxyanion hole of BChE via glycine interaction. The overlaid dock poses of all the synthesized compounds at both ChE enzymes were also depicted in Fig 6 to highlight their relative position as well as their helpful interaction.

BACE-1 is a membrane-bound enzyme with catalytic aspartic dyad residues at the N-terminus and C-terminus interfaces (Asp32

Table 2
In silico docking interaction analysis of compound 6f and donepezil on AChE (4EY7).

Comp.	Interacting residues[#]					
	CAS	PAS	Anionic sub-site	Acyl binding pocket	Oxyanion hole	Other interacting residues
6f	Ser203[a], His447[a]	Tyr72[c], Tyr124[c], Trp286[b,c], Tyr341[c], Asp74[d]	Trp86[b,c], Glu202[d]	Phe295[c], Phe338[c]	Phe297[c], Gly121[f]	Tyr133[c], Leu76[c], Val294[c], Tyr337[c], Gly448[f], Ile451[c], Thr75[a], His287[a]
Don*	Ser203[a], His447[a]	Tyr72[c], Tyr124[c], Trp286[b,c], Tyr341[c],	Trp86[b,c], Glu202[d]	Phe295[c], Phe338[c]	Phe297[c], Gly121[c]	Tyr133[c], Leu289[c], Val294[c], Tyr337[c], Gly448[c], Ile451[c]

[#] All the interacting residues are within the 4 A distance with the ligand;
[*] Don – Donepezil;
[a] –polar interaction;
[b] –π-π stacking interaction;
[c] –hydrophobic interaction;
[d] –charged interaction;
[e] –π-cation interaction;
[f] –glycine interaction;
[g] –hydrogen bonding.

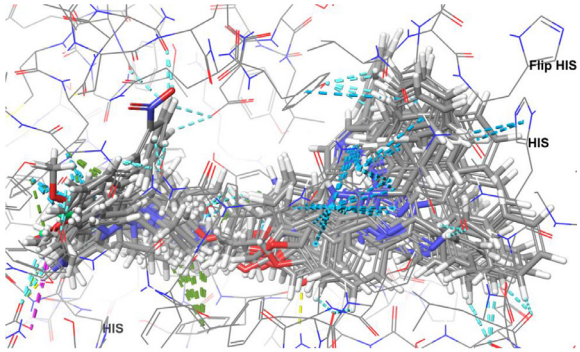

a)

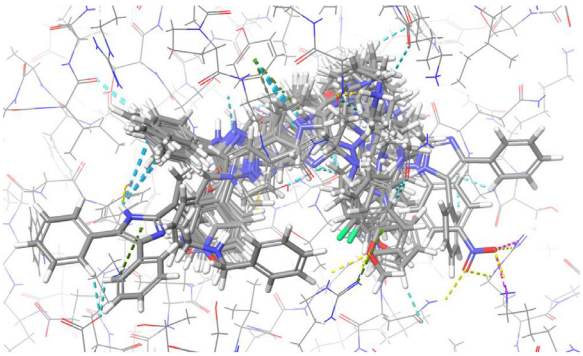

b)

Fig 6. The superimposed docking poses of all the synthesized compounds at a) AChE (PDB: 4EY7) b) BChE (PDB: 2ZJM)

and Asp228). Compound **6f** indicated charged interactions with the Asp228 residue of BACE-1(Fig. 7).

2.4.2. Molecular dynamics (MD) simulation

The molecular dynamics simulation study used Desmond (DE Shaw Research) to analyze the compound **6f**-AChE complex binding stability. The simulations of molecular dynamics evaluated the stability of the docked complex along with virtual water surrounding in a flexible protein. The values of the docked complexes' root mean square deviations (RMSD) were determined and compared to the reference protein backbone structures within the range. Root mean square fluctuations (RMSF) values for the compound **6f**-AChE complex showed stable ligand and protein residue trajectories during the simulation analysis. The detailed analysis of interaction was performed using the histogram, graphical, and time-line representation of the protein-ligand. Using protein-ligand contacts, the percentage of protein residue interactions with compound **6f** was identified. The findings of AChE molecular dynamics studies proposed that compound **6f** interacted considerably with PAS residues of AChE (Fig. 7). At the PAS region, the Trp286 residue created π-π stacking (62% time-scale) and hydrophobic interactions with imidazole moiety of compound **6f**. Also, the Tyr341 residue formed the same interactions as that of Trp286 residue with compound **6f** in the PAS region for a 70% time-scale. Asp74, a PAS residue that interacted with the nitrogen atom (N-1) of piperazine ring of compound **6f** through the creation of salt bridge (47% time-scale) and charged interaction. The piperazine nitrogen atom (N-1) and phenyl ring of benzyl piperazine moiety of compound **6f** displayed π-cation (80% time-scale) and π-π stacking interactions (49% time-scale) with Trp86 residue of the anionic subsite, respectively. At anionic subsite, Trp86 residue also exhibited hydrophobic interactions with the benzyl piperazine portion of compound **6f**. Other interacting residues, like His287, formed π-π stacking (31% time-scale) as well as polar interactions with diaryl part of the compound **6f**.

The results of the BACE-1 molecular dynamics simulation showed that Compound **6f** created nominal interactions with aspartate dyad residues (Asp32 and Asp228) with fluctuations. The MD findings suggested that compound **6f** showed more stable interaction in AChE as compared to BACE-1 (Fig. 7 and 8)

2.4.3. Drug-likeliness by QikProp module

The drug-likeliness properties of compound **6f** were assessed using Schrödinger's QikProp module, and the results were determined to be comparable to ordinary donepezil (Table 3). Lipinski's rule of five (mol MW 500, QPlog Po/w 5, donorHB 0–6.0, accptHB 2.0–20), as well as the other expected parameters (SASA 300–1000, QPlogBB 3.0 to 1.2, QPlogPo/w 2.0 to 6.5), indicated that compound **6f** elicited "drug-like" properties.

3. Conclusion

Continuing with the ideas of bioisosterism and hybrid pharmacophore and pursuance in the development of newer and safer agents as ChE and BACE-1, the substituted piperazine nucleus tethered with 4, 5-diaryl-1*H*-imidazole scaffold through different linkers were designed. The synthesized derivatives (**6a-g** and **7a-g**) were initially evaluated for ChE inhibition potential using Ellman's colorimetric protocol. Amongst the tested compounds, **6c, 6e**, and **6f** showed significant eeAChE inhibitory activity. Compound **6f** containing the benzyl piperazine moiety displayed most significant eeAChE (IC_{50} = 0.416 ± 0.018 μM) and eqBChE (IC_{50} = 0.474 ± 0.054 μM) inhibitory activity. Compound **6f** showed a potent BACE-1 (IC_{50} = 0.392 ± 0.021 μM) inhibitory potential. Compounds **6b, 6c, 6e**, and **6f** were evaluated for propidium iodide displacement

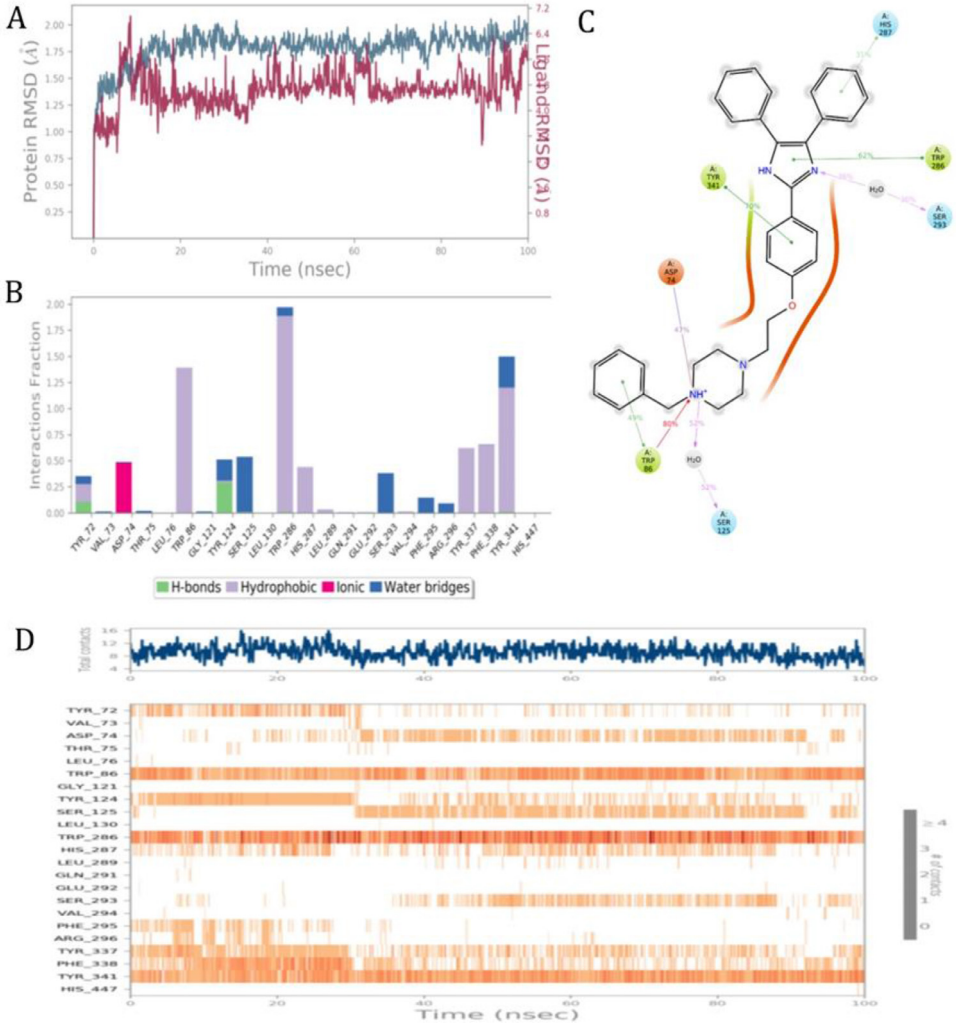

Fig. 7. Molecular dynamics studies of 6f-AChE (4EY7) docked complex. [A] RMSD graph of the compound 6f-AChE complex for the period of 100 ns dynamics simulations; [B] Interaction fractions of active amino acid residues are displayed in a histogram; [C] Graphical representation of compound 6f showing interacting residues for the simulations of 100 ns; [D] At each time frame, a timeline representation of interaction with all amino acid residues was displayed.

Table 3
QikProp analysis of compound 6f.

Compound	Mol_ Wt	Donor HB	Acceptor HB	SASA	QplogBB	Qplogo/w
Donepezil	393.61	1	7.1	759.67	0.14	4.25
6f	514.7	0	3.0	789.48	0.78	6.474

[a]Mol_MW- Molecular weight of the molecule (130 to 725).
[b]Donor HB- number of hydrogen bonds (0.0 to 6.0).
[c]Acceptor HB- number of hydrogen bonds (2.0 to 20.0).
[d]SASA- total solvent accessible surface area (SASA) in square angstroms using a probe with 1.4 A radius (300 to1000).
[e]QPlogBB- predicted brain/blood partition coefficient (-3.0 to 1.2).
[f]QPlogPo/w- this gives the predicted octanol/water partition coefficient (-2.0 to 6.5).

capability from PAS-AChE. Compound **6f** showed a greater propidium iodide displacement (10 μM = 29.09%, 50 μM = 41.43%) relative to donepezil (10 μM = 24.86%, 50 μM = 36.31%). The inhibitor (**6f**) exhibited greater anti-aggregatory property in self-induced (21.28 to 30.85%) and AChE-induced (25.70 to 51.07%) studies compared with donepezil (self-induced: 14.59 to 21.17%; AChE-induced: 19.72 to 33.05%). The *in-vivo* behavioral study revealed that the scopolamine group induces memory impairment in rats, in comparison to donepezil (5 mg/kg), compound **6f** (10 mg/kg) showed a statistically non-significant difference in percent spontaneous alterations. Compound **6f** was monitored for its binding affinity and binding pattern with an active site residue of AChE (PDB Code: 4EY7), BChE (PDB Code: 4TPK), and BACE-1 (2ZJM) by conducting molecular docking studies and found that compound **6f** significantly interact with all the respective enzymes. The stability of the compound **6f** was analyzed through a molecular dynamics simulation study and compound **6f** showed more stable interaction in AChE as compared to BACE-1. Based on overall outcomes, compound **6f** could be regarded as a prospective lead candidate in the management of AD.

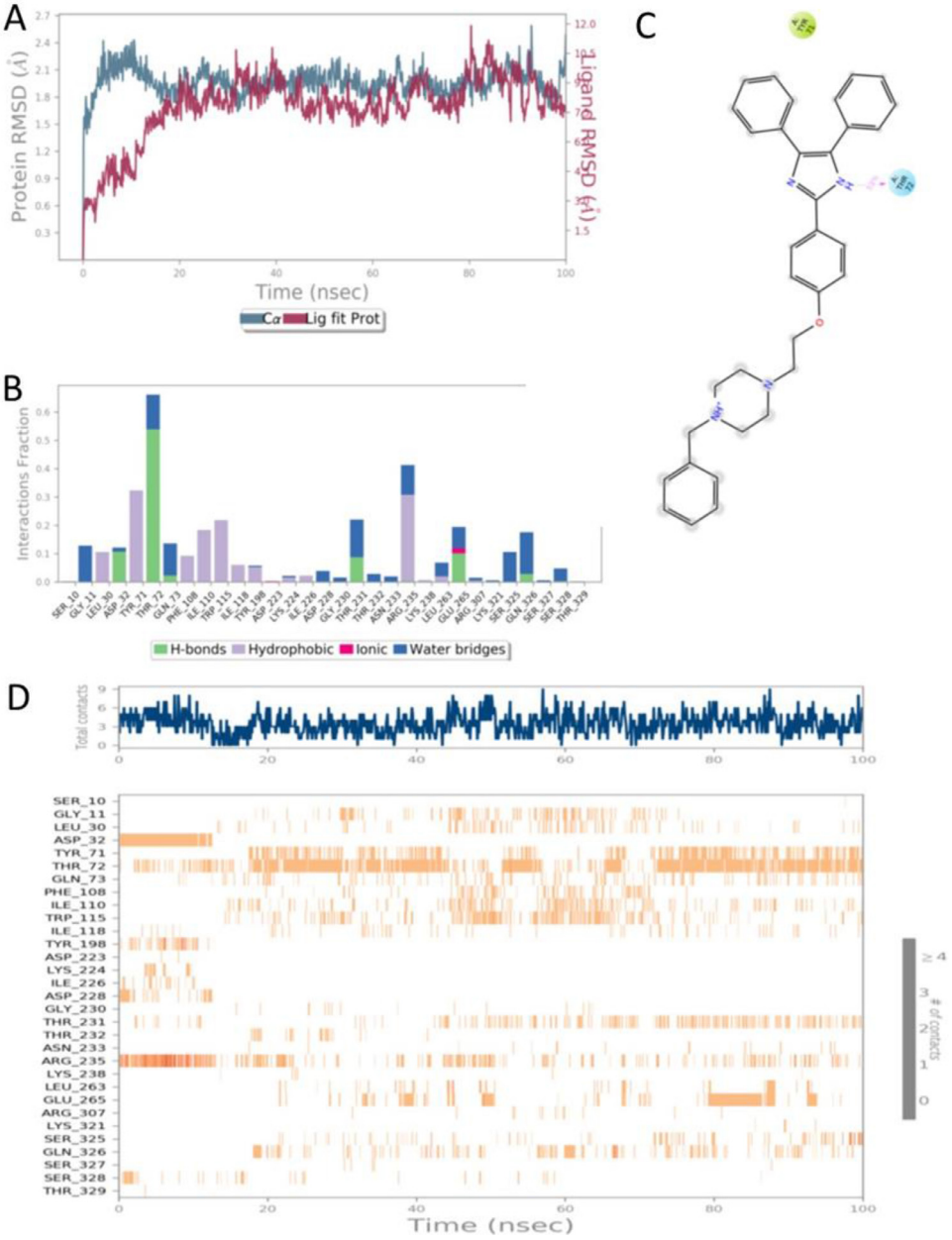

Fig. 8. Molecular dynamics studies of 6f-BACE-1 (2ZJM) docked complex. [A] RMSD graph of the compound 6f-BACE-1 complex for the period of 100 ns dynamics simulations; [B] Interaction fractions of active amino acid residues are displayed in a histogram; [C] Graphical representation of compound 6f showing interacting residues for the simulations of 100 ns; [D] At each time frame, a timeline representation of interaction with all amino acid residues was displayed.

4. Experimental

4.1. Chemistry

4.1.1. Instrumentation and chemicals

Avra Synthesis, TCI Chemicals, and Sigma Aldrich provided both reagents and chemicals (India). Progress of chemical reactions was monitored by using pre-coated aluminum sheets of silica gel 60 F254 of thickness 0.25 mm, (Merk, Germany), and the R_f values are also determined using the same sheets. The IR spectra (wave numbers in cm-1) were recorded on FT-IR spectrophotometer using potassium bromide discs. The melting points were calculated using capillary tubes and Stuart Melting Point apparatus (SMP10) using capillary tubes and listed as uncorrected. The Retention factor (Rf) values were determined using solvent system methanol: dichloromethane (2:98) to monitor the progress of the reaction. UV light, Dragendorff's reagent, vapors of iodine were used for visualization of TLC plates. FT-NMR spectrophotometer (Bruker Avance) was used to record ^{1}H NMR spectra (500 MHz) and ^{13}C NMR spectra (125 MHz) in DMSO-d_6 or $CDCl_3$ using tetramethylsilane as an internal standard, and the spectra were interpreted with the help of MestReNova version 6.0.2. The absorbance of inhibitors at different concentrations was measured colorimetrically at 412 nm using a Multimode Microplate Reader (BioTek Synergy H1M, USA). Using an Infinity II 1260 High-Performance Liquid Chromatography (Agilent, USA) with an Eclipse Plus C8 column and a methanol/water (90:10 v/v) mobile phase at a flow rate of 1 mL/min, the percent purity of synthesised compounds was determined to be $\geq$ 95%.

4.1.2. Synthesis

4.1.2.1. General procedure for the synthesis of intermediates 2, 3. Compound **1** (8.18 mmol) was dissolved in 15 mL ACN in a round

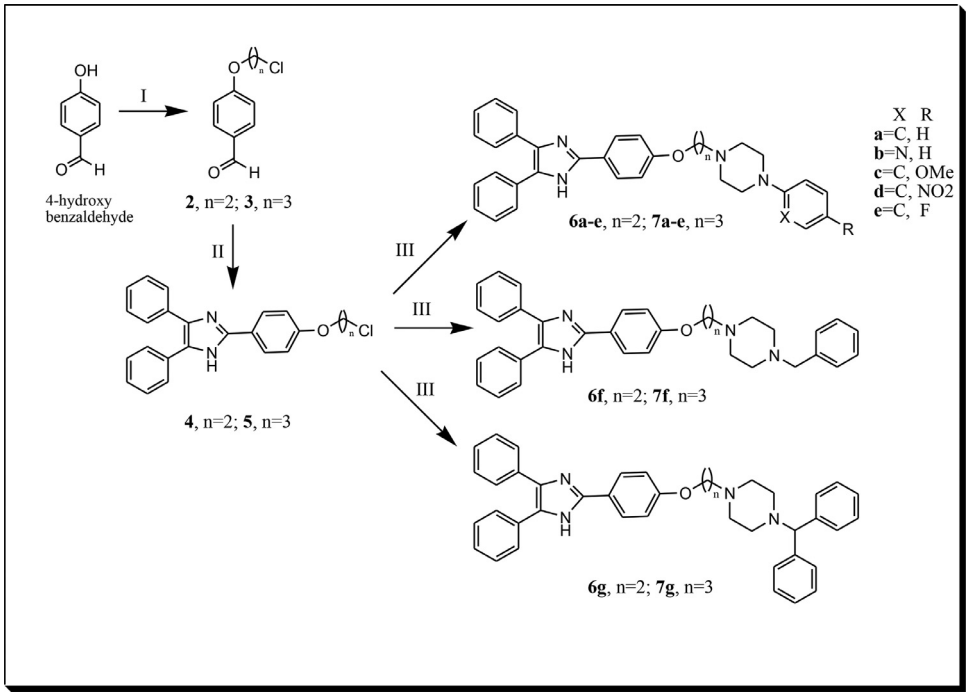

Scheme 1. Reagents and conditions: (I) anhydrous potassium carbonate, $Br(CH_2)_nCl$ (n = 2 and 3), ACN, reflux, 7-8 8 h; (II) benzoin, ammonium acetate, cerric ammonium nitrate, and ethanol:water, reflux (III) substituted piperazines, potassium iodide, anhydrous potassium carbonate, and ACN, reflux, 16 h.

bottom flask at room temperature. An accurate quantity of dry K_2CO_3 (10.63 mmol) was added, and after some time, compound **1** was precipitated in the form of potassium salt. Bromo chloro substituted alkane (8.18 mmol) (1, 2-dibromo ethane, 1, 3-bromochloro propane) were added to the reaction mixture and refluxed for 7-8 h. The reaction was completed and it was affirmed by TLC using ethyl acetate: hexane (20:80) as mobile phase. The ACN was evaporated under reduced pressure, the solid residue was obtained. This solid residue dissolved in ethyl acetate and washed with water followed by passing over anhydrous sodium sulfate. The organic layer was taken and evaporated under a vacuum. The crude product was obtained, which was then purified by using mobile phase ethyl acetate: hexane (1:99) and stationary phase silica gel through column chromatography to afford intermediates **2** and **3**.

4-(2-bromoethoxy) benzaldehyde (2)

^{1}H NMR (500 MHz, $\delta_{H,}$ $CDCl_3$): 9.88 (s, 1H), 7.84 (d, 2H, J = 8.8 Hz), 7.01 (d, 2H, J = 8.7 Hz), 4.36 (t, 2H, J = 6.2 Hz), 3.66 (t, 2H, J = 6.2 Hz). ^{13}C NMR (125 MHz, $\delta_{C,}$ $CDCl_3$): 190.71, 163.02, 132.04, 130.50, 114.90, 67.97, 28.48.

Anal. $C_9H_9BrO_2$: C,47.19; H,3.96; Br,34.88; O,13.97; Found: C,47.17; H,3.95; Br,34.86; O,13.98.

4-(3-chloropropoxy) benzaldehyde (3)

^{1}H NMR (500 MHz, $\delta_{H,}$ $CDCl_3$): 9.85 (s, 1H), 7.80 (d, 2H, J = 8.7 Hz), 6.98 (d, 2H, J = 8.7 Hz), 4.17 (t, 2H, J = 5.9 Hz), 3.72 (t, 2H, J = 6.3 Hz), 2.24 (p, 2H, J = 6.0 Hz). ^{13}C NMR (125 MHz, $\delta_{C,}$ $CDCl_3$): 190.82, 163.73, 132.01, 130.06, 114.77, 64.63, 41.24, 31.96.

Anal. $C_{10}H_{11}ClO_2$: C,60.46; H,5.58; Cl,17.85; O,16.11; Found: C,60.47; H,5.55; Cl,17.84; O,16.13.

4.1.2.2. General procedure for the synthesis of intermediates 4, 5. Ammonium acetate (14.08 mmol), cerric ammonium nitrate (0.35 mmol), and benzoin (3.52 mmol) were dissolved in a 10 ml mixture of ethanol:water (1:1, v/v). Intermediate **2** or **3** (3.52 mmol) was added to the above mixture and refluxed till the completion of the reaction, which was indicated by using TLC having ethyl acetate:hexane (40:60) as mobile phase. The solid get precipitated when the reaction mixture was added into ice-cold water after the cooling of the reaction mixture at room temperature. The solid was obtained by vacuum filtration, followed by water-washed and dried to give crude solid. Crude solid was purified by using mobile phase ethyl acetate:hexane (5:95) and stationary phase silica gel through column chromatography to afford intermediates **4** and **5**.

2-(4-(2-bromoethoxy)phenyl)-4, 5-diphenyl-1*H*-imidazole (4)

^{1}H NMR (500 MHz, $\delta_{H,}$ DMSO-d_6): 12.66 (s, 1H), 8.17 (d, 1H, J = 2.1 Hz), 8.01 (dd, 1H, J = 8.6, 3.2 Hz), 7.56 – 7.41 (m, 7H), 7.37 (t, 1H, J = 7.3 Hz), 7.31 (dd, 3H, J = 7.9, 6.8 Hz), 7.23 (t, 1H, J = 7.3 Hz), 4.50 – 4.45 (m, 2H), 3.89 – 3.85 (m, 2H). ^{13}C NMR (125 MHz, $\delta_{C,}$ DMSO-d_6): 153.23, 144.17, 130.98, 128.71, 128.33, 128.25, 127.12, 126.62, 121.79, 114.40, 68.85, 31.07.

Anal. $C_{23}H_{19}BrN_2O$: C,65.88; H,4.57; Br,19.06; N,6.68; O,3.82; Found: C,65.86; H,4.54; Br,19.09; N,6.64; O,3.79.

2-(4-(3-chloropropoxy)phenyl)-4, 5-diphenyl-1*H*-imidazole (5)

^{1}H NMR (500 MHz, $\delta_{H,}$ DMSO-d_6): 12.53 (s, 1H), 8.02 (d, 2H, J = 8.6 Hz), 7.77 – 7.15 (m, 10H), 7.06 (d, 2H, J = 8.7 Hz), 4.15 (t, 2H, J = 6.0 Hz), 3.82 (t, 2H, J = 6.4 Hz), 2.20 (p, 2H, J = 6.1 Hz). ^{13}C NMR (125 MHz, $\delta_{C,}$ DMSO-d_6): 158.54, 145.59, 128.20, 127.56, 127.46, 126.92, 126.60, 126.09, 123.31, 114.63, 64.36, 42.00, 31.73.

Anal. $C_{24}H_{21}ClN_2O$: C,74.12; H,5.44; Cl,9.12; N,7.20; O,4.11; Found: C,74.08; H,5.48; Cl,9.10; N,7.23; O,4.08.

4.1.2.3. General procedure for the synthesis of compounds 6a-g and 7a-g. 10 ml ACN was taken in a round bottom flask and intermediate **4** or **5** (1.19 mmol), potassium iodide (1.78 mmol), various substituted piperazines (1.19 mmol), and dry potassium carbonate (1.78 mmol) were suspended into it and refluxed for 16 h. Completion of the reaction was monitored by TLC using MeOH:DCM (2:98) as a mobile phase. The solvent was evaporated by the application of a rota evaporator to get the solid residue. The obtained solids were dissolved in ethyl acetate and washed with water. The residual water was removed with the help of dry sodium sulfate. The organic layer was vaporized using a rota evaporator to yield crude solid, which was purified by using mobile phase MeOH:DCM (2:98)

and stationary phase silica gel with the help of column chromatography to yield pure compounds **6a-g** and **7a-g**.

1-(2-(4-(4, 5-diphenyl-1*H*-imidazol-2-yl)phenoxy)ethyl)-4-phenylpiperazine (6a)

Yield: 71%; mp: 156-158 °C; R_f = 0.52 (MeOH:DCM, 2:98 v/v); IR (KBr, cm^{-1}): 3346, 3114, 1654, 1276, 1136; ^{1}H NMR (500 MHz, $\delta_{H,}$ $CDCl_3$): 12.50 (s, 1H), 7.85 (d, 2H, *J* = 8.7 Hz), 7.56 (d, 4H, *J* = 7.0 Hz), 7.35 (t, 4H, *J* = 7.4 Hz), 7.32 – 7.28 (m, 4H), 6.99 (d, 2H, *J* = 8.8 Hz), 6.95 (d, 2H, *J* = 8.0 Hz), 6.89 (t, 1H, *J* = 7.3 Hz), 4.21 (t, 2H, *J* = 5.7 Hz), 3.29 – 3.22 (m, 4H), 2.92 (t, 2H, *J* = 5.7 Hz), 2.81 – 2.76 (m, 4H). ^{13}C NMR (125 MHz, $\delta_{C,}$ $CDCl_3$): 159.31, 151.24, 146.06, 129.13, 128.58, 127.82, 127.59, 126.82, 122.97, 119.82, 116.13, 114.95, 66.01, 57.20, 53.69, 49.07.

Anal. $C_{33}H_{32}N_4O$: C,79.17; H,6.44; N,11.19; O,3.20; Found: C,79.21; H,6.47; N,11.15; O,3.17. HPLC purity: 99.19%, retention time: 3.147 min.

1-(2-(4-(4, 5-diphenyl-1*H*-imidazol-2-yl)phenoxy)ethyl)-4-(pyridin-2-yl)piperazine (6b)

Yield: 68%; mp: 157-159 °C; R_f = 0.52 (MeOH:DCM, 2:98 v/v); IR (KBr, cm^{-1}): 3352, 3090, 1662, 1682, 1273, 1128; ^{1}H NMR (500 MHz, $\delta_{H,}$ DMSO-d_6): 12.51 (s, 1H), 8.13 – 8.02 (m, 3H), 7.60 – 7.47 (m, 7H), 7.34 – 7.28 (m, 4H), 7.10 (d, 2H, *J* = 8.7 Hz), 6.76 – 6.58 (m, 2H), 4.09 (t, 2H, *J* = 6.4 Hz), 3.64 -3.51 (m, 4H), 3.13 – 2.94 (m, 4H), 2.75 (t, 2H, *J* = 6.5 Hz). ^{13}C NMR (125 MHz, $\delta_{C,}$ DMSO-d_6): 160.97, 157.83, 148.14, 145.89, 142.51, 139.65, 130.21, 129.27, 128.77, 127.87, 127.34, 126.73, 115.30, 114.01, 108.19, 67.76, 54.57, 52.66, 47.31.

Anal. $C_{32}H_{31}N_5O$: C,76.62; H,6.23; N,13.96; O,3.19; Found: C,76.64; H,6.27; N,13.93; O,3.16. HPLC purity: 95.47%, retention time: 3.173 min.

1-(2-(4-(4, 5-diphenyl-1*H*-imidazol-2-yl)phenoxy)ethyl)-4-(4-methoxyphenyl)piperazine

(6c)

Yield: 74%; mp: 162-164 °C; R_f = 0.52 (MeOH:DCM, 2:98 v/v); IR (KBr, cm^{-1}): 3428, 3092, 1664, 1283, 1269, 1147; ^{1}H NMR (500 MHz, $\delta_{H,}$ DMSO-d_6): 12.51 (s, 1H), 7.99 (d, 2H, *J* = 8.7 Hz), 7.56 – 7.47 (m, 6H), 7.39 – 7.28 (m, 4H), 7.01 (d, 2H, *J* = 8.7 Hz), 6.71 – 6.60 (m, 4H), 3.99 (t, 2H, J = 5.3 Hz), 3.59 (s, 3H), 3.13 (t, 4H, *J* = 5.5 Hz), 2.90 (t, 4H, *J* = 5.3 Hz), 2.32 (t, 2H, *J* = 5.3 Hz). ^{13}C NMR (125 MHz, $\delta_{C,}$ DMSO-d_6): 159.16, 152.88, 145.21, 143.56, 130.13, 129.39, 128.67, 127.78, 127.47, 127.28, 126.66, 126.18, 116.07, 114.98, 66.37, 55.93, 54.63, 52.56, 49.02.

Anal. $C_{34}H_{34}N_4O_2$: C,76.95; H,6.46; N,10.56; O,6.03; Found: C,76.94; H,6.49; N,10.53; O,6.07. HPLC purity: 99.83%, retention time: 2.613 min.

1-(2-(4-(4, 5-diphenyl-1*H*-imidazol-2-yl)phenoxy)ethyl)-4-(4-nitrophenyl)piperazine (6d)

Yield: 76%; mp: 164-166 °C; R_f = 0.52 (MeOH:DCM, 2:98 v/v); IR (KBr, cm^{-1}): 3323, 3124, 1523, 1649, 1354, 1271, 1128; ^{1}H NMR (500 MHz, $\delta_{H,}$ DMSO-d_6): 12.48 (s, 1H), 8.09 – 7.92 (m, 4H), 7.63 –7.36 (m, 10H), 7.10 – 6.89 (m, 4H), 4.17 (t, 2H, *J* = 5.6 Hz), 3.40 (t, 4H, *J* = 5.7 Hz), 3.32 – 2.94 (m, 4H), 2.73 (t, 2H, *J* = 5.6 Hz). ^{13}C NMR (125 MHz, $\delta_{C,}$ DMSO-d_6): 160.87, 157.12, 145.47, 143.51, 137.24, 130.45, 129.33, 128.79, 127.87, 127.25, 126.83, 126.30, 114.89, 112.65, 67.76, 54.26, 52.58, 49.12.

Anal. $C_{33}H_{31}N_5O_3$: C,72.64; H,5.73; N,12.84; O,8.80; Found: C,72.67; H,5.70; N,12.85; O,8.78. HPLC purity: 96.80%, retention time: 3.360 min.

1-(2-(4-(4, 5-diphenyl-1*H*-imidazol-2-yl)phenoxy)ethyl)-4-(4-fluorophenyl)piperazine (6e)

Yield: 73%; mp: 162-164 °C; R_f = 0.52 (MeOH:DCM, 2:98 v/v); IR (KBr, cm^{-1}): 3344, 3132, 1645, 1323, 1267, 1163; ^{1}H NMR (500 MHz, $\delta_{H,}$ DMSO-d_6): 12.50 (s, 1H), 8.03 (d, 2H, *J* = 8.6 Hz), 7.61 – 7.43 (m, 6H), 7.31 – 7.24 (m, 4H), 7.11 – 6.96 (m, 4H), 6.67 (d, 2H, *J* = 8.6 Hz), 4.10 (t, 2H, *J* = 5.8 Hz), 3.49 (t, 4H, *J* = 5.6 Hz), 2.83 (t, 4H, *J* = 5.7 Hz), 2.68 (t, 2H, *J* = 5.8 Hz). ^{13}C NMR (125 MHz, $\delta_{C,}$ DMSO-d_6): 160.01(d, *J* C-F = 224.2 Hz), 158.52, 149.21, 145.09, 130.71, 129.57, 128.47, 127.97, 127.19, 126.82, 126.23, 118.11, 117.33, 114.97, 68.13, 55.48, 51.24, 49.37.

Anal. $C_{34}H_{33}FN_4O$: C,76.42; H,6.03; F,3.66; N,10.80; O,3.08; Found: C,76.39; H,6.05; F,3.3.67; N,10.82; O,3.07. HPLC purity: 97.54%, retention time: 3.613 min.

1-benzyl-4-(2-(4-(4, 5-diphenyl-1*H*-imidazol-2-yl)phenoxy)ethyl)piperazine (6f)

Yield: 69%; mp: 158-160 °C; R_f = 0.52 (MeOH:DCM, 2:98 v/v); IR (KBr, cm^{-1}): 3344, 3119, 1648, 1281, 1129; ^{1}H NMR (500 MHz, $\delta_{H,}$ $CDCl_3$): 12.49 (s, 1H), 7.85 (d, 2H, *J* = 8.8 Hz), 7.57 (d, 4H, *J* = 7.1 Hz), 7.35 – 7.27 (m, 11H), 6.95 (d, 2H, *J* = 8.8 Hz), 4.16 (t, 2H, *J* = 5.5 Hz), 3.56 (s, 2H), 2.87 (t, 2H, *J* = 5.5 Hz), 2.68 – 2.56 (m, 8H). ^{13}C NMR (125 MHz, $\delta_{C,}$ $CDCl_3$): 159.21, 146.07, 129.37, 128.56, 128.31, 127.83, 127.30, 126.82, 123.00, 114.89, 65.76, 62.82, 57.03, 53.37, 52.62, 29.70.

Anal. $C_{34}H_{34}N_4O$: C,79.35; H,6.66; N,10.89; O,3.11; Found: C,79.32; H,6.65; N,10.87; O,3.09. HPLC purity: 96.52%, retention time: 4.653 min.

1-benzhydryl-4-(2-(4-(4, 5-diphenyl-1*H*-imidazol-2-yl)phenoxy)ethyl)piperazine (6g)

Yield: 72%; mp: 167-169 °C; R_f = 0.52 (MeOH:DCM, 2:98 v/v); IR (KBr, cm^{-1}): 3349, 3123, 1655, 1269, 1147; ^{1}H NMR (500 MHz, $\delta_{H,}$ DMSO-d_6): 12.50 (s, 1H), 8.07 – 7.92 (m, 2H), 7.55 –7.45 (m, 10H), 7.31 –7.12 (m, 10H), 7.05 – 6.97 (m, 2H), 5.18 (s, 1H), 4.21 (t, 2H, *J* = 5.7 Hz), 3.11 (t, 2H, *J* = 5.7 Hz), 2.71 – 2.52 (m, 8H). ^{13}C NMR (125 MHz, $\delta_{C,}$ DMSO-d_6): 159.93, 146.17, 142.91, 137.33, 130.35, 129.75, 129.42, 128.57, 127.99, 127.54, 127.13, 126.87, 126.33, 114.91, 77.04, 67.19, 55.57, 53.67, 51.01.

Anal. $C_{40}H_{38}N_4O$: C,81.32; H,6.48; N,9.48; O,2.71; Found: C,81.29; H,6.46; N,9.45; O,2.74. HPLC purity: 99.90%, retention time: 4.053 min.

1-(3-(4-(4, 5-diphenyl-1*H*-imidazol-2-yl)phenoxy)propyl)-4-phenylpiperazine (7a)

Yield: 66%; mp: 158-160 °C; R_f = 0.52 (MeOH:DCM, 2:98 v/v); IR (KBr, cm^{-1}): 3339, 3110, 1648, 1269, 1129; ^{1}H NMR (500 MHz, $\delta_{H,}$ $CDCl_3$): 12.49 (s, 1H), 7.95 (d, 2H, *J* = 8.8 Hz), 7.58 – 7.54 (m, 4H), 7.32 (t, 4H, *J* = 7.4 Hz), 7.27 (d, 4H, *J* = 5.9 Hz), 6.97 (d, 2H, *J* = 8.7 Hz), 6.93 (d, 3H, *J* = 7.9 Hz), 4.12 – 4.09 (m, 2H), 3.31 – 3.28 (m, 4H), 2.82 (dd, 6H, *J* = 15.8, 11.5 Hz), 2.15 – 2.11 (m, 2H). ^{13}C NMR (125 MHz, $\delta_{C,}$ $CDCl_3$): 162.29, 140.57, 129.38, 128.77, 128.08, 127.57, 120.46, 116.56, 115.01, 66.39, 55.25, 53.25, 48.81, 26.17.

Anal. $C_{34}H_{34}N_4O$: C,79.35; H,6.66; N,10.89; O,3.11; Found: C,79.38; H,6.69; N,10.87; O,3.13. HPLC purity: 96.44%, retention time: 5.733 min.

1-(3-(4-(4, 5-diphenyl-1*H*-imidazol-2-yl)phenoxy)propyl)-4-(pyridin-2-yl)piperazine (7b)

Yield: 70%; mp: 158-160 °C; R_f = 0.52 (MeOH:DCM, 2:98 v/v); IR (KBr, cm^{-1}): 3347, 3115, 1653, 1659, 1265, 1139; ^{1}H NMR (500 MHz, $\delta_{H,}$ $CDCl_3$): 12.50 (s, 1H), 8.18 (d, 1H, *J* = 3.3 Hz), 7.83 (d, 2H, *J* = 8.5 Hz), 7.59 – 7.45 (m, 6H), 7.32 (t, 4H, *J* = 7.4 Hz), 7.28 (s, 1H), 6.94 (d, 2H, *J* = 8.6 Hz), 6.64 (dd, 2H, *J* = 10.5, 6.1 Hz), 4.06 (t, 2H, *J* = 6.2 Hz), 3.59 – 3.54 (m, 4H), 2.62 (t, 6H, *J* = 7.1 Hz), 2.08 – 2.00 (m, 2H). ^{13}C NMR (125 MHz, $\delta_{C,}$ $CDCl_3$): 159.69, 148.15, 146.40, 137.80, 128.80, 128.06, 127.56, 127.08, 122.89, 115.03, 113.72, 107.43, 66.39, 55.40, 53.16, 45.22, 26.66.

Anal. $C_{33}H_{33}N_5O$: C,76.87; H,6.45; N,13.58; O,3.10; Found: C,76.89; H,6.42; N,13.57; O,3.12. HPLC purity: 97.13%, retention time: 3.387 min.

1-(3-(4-(4,5-diphenyl-1*H*-imidazol-2-yl)phenoxy)propyl)-4-(4-methoxyphenyl)piperazine (7c)

Yield: 62%; mp: 161-163 °C; R_f = 0.45 (MeOH:DCM, 2:98 v/v); IR (KBr, cm^{-1}): 3338, 3119, 1656, 1284, 1279, 1144; ^{1}H NMR (500 MHz, $\delta_{H,}$ DMSO-d_6): 12.51 (s, 1H), 8.01 (d, 2H, *J* = 8.5 Hz), 7.50 (d, 4H, *J* = 7.4 Hz), 7.31 (d, 6H, *J* = 35.7 Hz), 7.04 (d, 2H, *J* = 8.6 Hz), 6.89 (d, 2H, *J* = 8.9 Hz), 6.81 (d, 2H, *J* = 8.9 Hz), 4.08 (t, 2H,

J = 5.6 Hz), 3.66 (s, 3H), 3.09 (s, 4H), 2.80 (d, 6H, J = 22.7 Hz), 2.01 (s, 2H). ^{13}C NMR (125 MHz, $\delta_{H,}$ DMSO-d_6): 158.88, 153.34, 145.88, 144.98, 128.64, 127.89, 127.02, 123.27, 117.77, 114.84, 114.84, 65.77, 55.37, 54.19, 52.47, 48.84, 25.41.

Anal. $C_{35}H_{36}N_4O_2$: C,77.18; H,6.66; N,10.29; O,5.87; Found: C,77.15; H,6.69; N,10.25; O,5.84. HPLC purity: 97.89%, retention time: 3.440 min.

1-(3-(4-(4, 5-diphenyl-1*H*-imidazol-2-yl)phenoxy)propyl)-4-(4-nitrophenyl)piperazine (7d)

Yield: 71%; mp: 162-164 °C; R_f = 0.39 (MeOH:DCM, 2:98 v/v); IR (KBr, cm^{-1}): 3336, 3109, 1648, 1549, 1338, 1267, 1129; ^{1}H NMR (500 MHz, $\delta_{H,}$ DMSO-d_6): 12.49 (s, 1H), 8.11 (d, 2H, J = 8.6 Hz), 7.97 (d, 2H, J = 7.4 Hz), 7.54 –7.51 (m, 6H), 7.31 – 7.26 (m, 4H), 7.02 (d, 2H, J = 8.7 Hz), 6.87 (d, 2H, J = 7.5 Hz), 4.09 (t, 2H, J = 5.7 Hz), 3.35 – 3.27 (m, 4H), 3.27 – 2.84 (m, 6H), 2.03 (t, 2H, J = 5.7 Hz). ^{13}C NMR (125 MHz, $\delta_{C,}$ DMSO-d_6): 160.59, 157.65, 145.71, 143.40, 137.52, 130.79, 129.19, 128.46, 127.88, 127.37, 126.53, 125.35, 115.58, 112.47, 67.17, 53.46, 52.28, 50.30, 28.17.

Anal. $C_{34}H_{33}N_5O_3$: C,72.97; H,5.94; N,12.51; O,8.58; Found: C,73.00; H,5.96; N,12.49; O,8.56. HPLC purity: 99.82%, retention time: 2.933 min.

1-(3-(4-(4, 5-diphenyl-1*H*-imidazol-2-yl)phenoxy)propyl)-4-(4-fluorophenyl)piperazine (7e)

Yield: 69%; mp: 161-163 °C; R_f = 0.53 (MeOH:DCM, 2:98 v/v); IR (KBr, cm^{-1}): 3344, 3124, 1651, 1332, 1271, 1139; ^{1}H NMR (500 MHz, $\delta_{H,}$ DMSO-d_6): 12.48 (s, 1H), 7.98 (d, 2H, J = 8.7 Hz), 7.50 – 7.27 (m, 10H), 6.77 – 6.89 (m, 4H), 6.51 (d, 2H, J = 8.6 Hz), 4.02 (t, 2H, J = 5.7 Hz), 3.28 – 3.14 (m, 4H), 2.78 – 2.53 (m, 6H), 1.99 (t, 2H, J = 5.7 Hz). ^{13}C NMR (125 MHz, $\delta_{C,}$ DMSO-d_6): 160.30 (d, J C-F = 228.7 Hz), 157.98, 148.87, 145.29, 130.52, 129.77, 128.52, 127.84, 127.15, 126.84, 125.99, 118.23, 116.18, 115.07, 67.74, 53.00, 52.78, 51.21, 27.48.

Anal. $C_{34}H_{33}FN_4O$: C,76.67; H,6.24; F,3.57; N,10.52; O,3.00; Found: C,76.69; H,6.21; F,3.55; N,10.50; O,3.03. HPLC purity: 98.85%, retention time: 3.680 min.

1-benzyl-4-(3-(4-(4, 5-diphenyl-1*H*-imidazol-2-yl)phenoxy)propyl)piperazine (7f)

Yield: 72%; mp: 163-165 °C; R_f = 0.42 (MeOH:DCM, 2:98 v/v); IR (KBr, cm^{-1}): 3345, 3122, 1661, 1281, 1132; ^{1}H NMR (500 MHz, $\delta_{H,}$ DMSO-d_6): 12.50 (s, 1H), 8.02 (d, 2H, J = 8.7 Hz), 7.49 – 7.47 (m, 6H), 7.29 –7.28 (m, 5H), 7.24 – 7.21 (m, 4H), 7.01 (d, 2H, J = 8.7 Hz), 4.15 (t, 2H, J = 5.7 Hz), 3.54 (s, 2H), 2.47 (t, 2H, J = 5.8 Hz), 2.51 – 2.49 (m, 8H), 2.05 – 1.99 (m, 2H). ^{13}C NMR (125 MHz, $\delta_{C,}$ DMSO-d_6): 160.16, 145.82, 143.39, 138.72, 130.15, 129.79, 128.78, 128.43, 127.83, 127.45, 127.33, 126.24, 126.07, 115.59, 67.20, 63.72, 53.51, 52.46, 28.14.

Anal. $C_{35}H_{36}N_4O$: C,79.50; H,6.86; N,10.60; O,3.03; Found: C,79.53; H,6.82; N,10.57; O,3.06. HPLC purity: 98.98%, retention time: 3.880 min.

1-benzhydryl-4-(3-(4-(4, 5-diphenyl-1*H*-imidazol-2-yl)phenoxy)propyl)piperazine (7g)

Yield: 67%; mp: 167-169 °C; R_f = 0.61 (MeOH:DCM, 2:98 v/v); IR (KBr, cm^{-1}): 3334, 3121, 1663, 1268, 1128; ^{1}H NMR (500 MHz, $\delta_{H,}$ DMSO-d_6): 12.51 (s, 1H), 8.07 (d, 2H, J = 8.7 Hz), 7.54 – 7.48 (m, 10H), 7.28 –7.27 (m, 4H), 7.24 – 7.23 (m, 6H), 7.05 (d, 2H, J = 8.7 Hz), 5.15 (s, 1H), 4.18 (t, 2H, J = 5.6 Hz), 2.71 (t, 2H, J = 5.7 Hz), 2.67 – 2.59 (m, 4H), 2.53 – 2.47 (m, 4H), 2.12 – 2.03 (m, 2H). ^{13}C NMR (125 MHz, $\delta_{C,}$ DMSO-d_6): 159.96, 145.06, 143.44, 140.68, 130.95, 129.29, 129.18, 128.35, 127.83, 127.48, 127.40, 126.73, 126.57, 114.49, 77.67, 67.25, 53.65, 52.52, 52.28, 28.11.

Anal. $C_{41}H_{40}N_4O$: C,81.42; H,6.67; N,9.26; O,2.65; Found: C,81.45; H,6.70; N,9.23; O,2.68. HPLC purity: 98.97%, retention time: 5.667 min.

4.2. Pharmacology

4.2.1. In vitro *studies*

4.2.1.4. Cholinesterase inhibition assay (eeAChE and eqBChE). Targeted compounds were evaluated for their cholinesterase inhibitory potency against eeAChE and eqBChE as per the Ellman method [43]. Thiolated substrates are specifically hydrolyzed into thiocholine by the ChE enzyme. 5, 5-dithio-bis-(2-nitrobenzoic acid) (DTNB) is reduced by thiocholine results in the formation of the yellow color compound which can be identified colorimetrically at 412 nm. All the inhibitors were dissolved in DMSO, and eight rising concentrations of inhibitors were prepared. The eeAChE from electrophorus electricus (electric eel) and eqBChE from equine serum were purchased from Sigma Aldrich India. 2.5 U/ml solution of cholinesterase was prepared in Tris buffer pH 8. The solution of cholinesterase enzyme (eeAChE & eqBChE) (25 μL) and inhibitors of different concentrations (10 μL) were taken into a 96-well microplate and incubated for 10 min. Further, DTNB (40 μL) (1 mM), acetylthiocholine iodide (ATCI) or butyrylthiocholine iodide (BTCI) substrate (10 μL) (7.5 mM), and Tris buffer pH 8 (240 μL) were added into above microplate. The absorbance was measured at 412 nm wavelength. The rate of non-enzymatic reaction was assessed by a blank assay contains all components except AChE and BChE. The change in reaction rate and percent inhibitory potency of inhibitors were assessed. The assay was performed in triplicate, and Graph Pad Prism 5.01 was used to calculate the IC_{50} values of inhibitors [44].

4.2.1.5. BACE-1 inhibition assay. A FRET-based BACE-1 activity detection kit was used to evaluate all of the compounds for their BACE-1 inhibitory potency. The assay involved the breaking of the substrate by BACE-1, resulted in an increase in the fluorescent signal, and was done following the protocol given by the manufacturer. The detection kit includes human BACE-1 enzyme, stop solution, BACE-1 substrate (7-Methoxycoumarin-4-acetyl-[Asn670, Leu671]-Amyloid β/A4 precursor protein 770 fragments 667-676-(2, 4-dinitrophenyl) Lys-Arg-Arg amide trifluoroacetate salt), fluorescent assay buffer, and assay standard. Inhibitors with various concentrations were used, likely to suppress enzymes in a particular range of 20-80%. The intensity of fluorescence was immediately monitored after the BACE-1 enzyme was introduced, with the excitation and emission wavelengths set at 320 and 405 nm, respectively. Plates were incubated for about 2 h at 37°C and Multimode Microplate Reader was used to record the intensity of fluorescence. Following expression were used to determine the% inhibition: [(IFo-IFi)/IFo] × 100, where IFi and IFo are the intensities of fluorescence obtained with or without the presence of inhibitor, respectively, and linear regression graph (Graph Pad Prism 5.1) were used to calculate the IC_{50} values.

4.2.1.6. Propidium iodide displacement assay. Propidium iodide is tending to bind to the peripheral active site of eeAChE, where the eeAChE inhibitor competitively displaces the propidium iodide. This displacement was measured by the propidium iodide displacement assay to determine the capability of binding of inhibitors to the PAS of eeAChE. The solution of eeAChE enzyme (5 U) in tris buffer pH 8.0 was prepared. Various test compounds with different concentrations were incorporated into the solution and incubated for 6 h at 25 °C. Propidium iodide was added after incubation, and fluorescence was measured at wavelengths of 535 nm (excitation) and 595 nm (emission) after 10 minutes.

4.2.1.7. Aβ inhibition- thioflavin T assay. The compound **6f** was tested for the AChE-induced A$\beta_{1\text{-}42}$ aggregation inhibitory activity by the thioflavin T assay. 2000 mM stock solution was obtained by dissolving A$\beta_{1\text{-}42}$ in 1% v/v solution of ammonium hydroxide and stored at 80°C. Initially, DMSO was used to dissolve the test compounds, and further dilutions were prepared using PBS pH 7.4. For self-induced A$\beta_{1\text{-}42}$ aggregation inhibition experiment, A$\beta_{1\text{-}42}$

(10 μM, 10 ml) were incubated for 48 h at 37°C in the presence or absence of inhibitor (5 μM, 10 μM, and 20 μM; 10 ml). Blank assays were carried out without A$\beta_{1\text{-}42}$, only with PBS pH 7.4 in the presence or absence of inhibitor. Thioflavin T (5 μM) in the glycine-NaOH buffer (50 μM) pH 8.0 was added to the assay mixture and intensities of fluorescence were measured at excitation and emission wavelengths of 485 nm and 528 nm, respectively. Following expression were used to determine the % inhibition of self-induced A$\beta_{1\text{-}42}$ aggregation: (IFc-IFi/IFc) $\times$ 100, where IFi and IFc are the intensities of fluorescence found with or without the presence of inhibitor, respectively. Every experiment was executed in triplicates. For the A$\beta_{1\text{-}42}$ AChE-induced aggregation inhibition experiment, A$\beta_{1\text{-}42}$ (10 μM, 2 ml) and AChE (230 μM, 16 ml) were incubated for 48 h at 37°C with or without the presence of inhibitor (5 μM, 10 μM, and 20 μM; 2 ml).

4.2.2. In vivo *studies*

4.2.2.8. Animals. The rats of either sex having weight 220-270 g of both the sexes were obtained from the Institute of Medical Sciences (IMS), Banaras Hindu University (BHU), Varanasi. They were kept in a polyacrylic cage in a group of six per cage, a balanced diet and water were provided. Temperature condition (25 $\pm$ 2°C) and relative humidity (55 $\pm$ 10%) were maintained for rats with light/dark cycles for 12 h. The Committee on Institutional Animal Ethics (Dean/2017/CAEC/93) approved the study protocol.

4.2.2.9. Cognition enhancement testing in rats by using scopolamine-induced amnesia model. The solution of scopolamine hydrobromide was prepared in sterilized normal saline. Test compound **6f** and donepezil (standard) were dissolved in 0.3% w/v solution of sodium carboxymethyl cellulose. The rats were grouped as control, scopolamine, donepezil, and **6f**. Each group contains six animals. Donepezil and **6f** were administered orally queue die to the animal groups for seven days. Only 0.3% w/v solution of sodium carboxymethyl cellulose was given as a vehicle for scopolamine group rats.

4.2.2.10. Y-maze test. The Y-maze apparatus comprises 3 arms maze. Instant and short working memory was estimated with the help of this apparatus. After 30 min of the treatment on the seventh day, all animals were injected with scopolamine hydrobromide intra-peritoneally except the control group. The rats were independently placed at the center of the maze. In the beginning, the rats were often going into the arm of facing, so the first entry was deleted from the calculations. The spontaneous alternations and total arm entries were recorded for about 8 min. The memory betterment score was estimated by using following expression, percent spontaneous alteration = [number of spontaneous alternations / (total arm entries-2)] $\times$ 100 [45].

4.3. Computational studies

4.3.1. In-silico *docking simulations*

The study of molecular docking was conducted to evaluate the binding nature and interactions of the active site for compound **6f** on AChE (PDB Code: 4EY7), BChE (PDB Code:4TPK), and BACE-1 (PDB Code: 2ZJM) [46]. The protein's structure was processed by utilizing the Protein Preparation Wizard module. Hydrogen was initially incorporated and partial charges were allocated by utilizing the force field OPLS-2005. Using Prime the missing side chains and loops were incorporated. The water molecules from the heteroatoms with a range greater than 5 Å were extracted, and hetero atom states were generated using the Epik at pH 7.0. Besides, the PROPKA method was used to optimize the protein structure at pH 7.0 and minimized by maintaining the convergence heavy RMSD atoms at 0.30 Å at a restricted minimization. For receptor grid generation, the prepared co-crystallized protein structure was used to determine the active sites present in the 10 $\times$ 10 $\times$ 10 Å distance from the centric co-crystallized ligand (donepezil). By utilizing the LigPrep module, the generation of stable conformers (compound **6f** and donepezil) was incorporated, further which was docked using Schrodinger Maestro's Glide module 2018–1. A thorough assessment of interactions was carried out using the Glide XP visualizer tool.

4.3.2. Molecular dynamics

To confirm the binding strength and pattern of the compound **6f**-AChE and **6f**-BACE-1 complex using Desmond, a molecular dynamics simulation run of 100 ns was conducted. The clear-cut water environment was created by soaking the ligand-protein complex in the TIP3P molecules of water encompassed by the orthorhombic water box. The prepared complex system was neutralized by adding the necessary counter ions, and the isosmotic salt environment was maintained by adding 0.15 M NaCl. The system's energy minimization was achieved by using a combined gradient algorithm with maximal 2000 interactions with convergence criteria of 1 kcal/mol/A. Simulation run of 100 ns with periodic boundary conditions under isothermal-isobaric ensemble (NPT) was performed after energy minimization, and the system temperature and pressure were set respectively at 300 K and 1,013 atmospheric bar.

4.3.3. In silico *determination of drug-like properties*

Using Schrodinger Maestro's QikProp module 2018–1, the features of drug-likeliness were discovered. The properties of drug-likeliness in the molecule were determined by predicting many descriptors, such as QPlogBB, PSA (polar surface area), and others, using Lipinski's rule of five (accept HB $\leq$10, donor HB $<$ 5, QPlogPo/w $<$ 5, mol MW $<$ 500).

4.4. Statistical analysis

The values are displayed as Mean $\pm$ SEM for each experimental group. One-way ANOVA or two-way ANOVA was used by statistical analysis software (Graph Pad Software, Inc., San Diego, CA) to evaluate differences between two groups (study and test).

Credit author statement

Salunke Prashant Ramrao: His research contribution includes planning, carried out the experiments, design, synthesis, and characterization, in-vitro evaluation of novel molecules.

Akash Verma: His research contribution includes rationale designing, writing, analyze the data, in-vitro evaluations of novel molecules.

Prabhash Nath Tripathi: His research contribution includes rationale designing, and in-vivo evaluation.

Digambar Kumar Waiker: His research contribution includes rationale designing, writing, in-silico estimation of various novel molecules.

Sushant Kumar Shrivastava (Co-Author): His research contribution includes planning, supervised the work, rationale designing, characterization, writing, biological evaluation of various molecules.

Declaration of Competing Interest

The authors declare that they have no known competing financial interests or personal relationships that could have appeared to influence the work reported in this paper.

Acknowledgement

For conducting NMR experiments, the authors gratefully acknowledge the Central Instrument Facility (CIF), Indian Institute of Technology (Banaras Hindu University), Varanasi.

References

[1] P.J. Gallaway, et al., Physical activity: a viable way to reduce the risks of mild cognitive impairment, Alzheimer's disease, and vascular dementia in older adults, Brain Sci. 7 (2) (2017) 22.
[2] C. Patterson, The State of the Art of Dementia Research: New Frontiers, 2018 World Alzheimer Report.
[3] P.N. Tripathi, et al., Biphenyl-3-oxo-1, 2, 4-triazine linked piperazine derivatives as potential cholinesterase inhibitors with anti-oxidant property to improve the learning and memory, Bioorg. Chem. 85 (2019) 82–96.
[4] N. Tabet, Acetylcholinesterase inhibitors for Alzheimer's disease: anti-inflammatories in acetylcholine clothing!, Age Ageing 35 (4) (2006) 336–338.
[5] H. Oakley, et al., Intraneuronal β-amyloid aggregates, neurodegeneration, and neuron loss in transgenic mice with five familial Alzheimer's disease mutations: potential factors in amyloid plaque formation, J. Neurosci. 26 (40) (2006) 10129–10140.
[6] D. Olivares, et al., N-methyl D-aspartate (NMDA) receptor antagonists and memantine treatment for Alzheimer's disease, vascular dementia and Parkinson's disease, Curr. Alzheimer Res. 9 (6) (2012) 746–758.
[7] R.B. Maccioni, et al., The revitalized tau hypothesis on Alzheimer's disease, Arch. Med. Res. 41 (3) (2010) 226–231.
[8] M.T. Heneka, et al., Neuroinflammation in Alzheimer's disease, Lancet Neurol. 14 (4) (2015) 388–405.
[9] E. Giacobini, Cholinesterases: new roles in brain function and in Alzheimer's disease, Neurochem. Res. 28 (3–4) (2003) 515–522.
[10] M. Bartolini, et al., β-Amyloid aggregation induced by human acetylcholinesterase: inhibition studies, Biochem. Pharmacol. 65 (3) (2003) 407–416.
[11] N.C. Inestrosa, et al., Acetylcholinesterase accelerates assembly of amyloid-β-peptides into Alzheimer's fibrils: possible role of the peripheral site of the enzyme, Neuron 16 (4) (1996) 881–891.
[12] V.Y. Hook, T.D. Reisine, Cysteine proteases are the major β-secretase in the regulated secretory pathway that provides most of the β-amyloid in Alzheimer's disease: role of BACE 1 in the constitutive secretory pathway, J. Neurosci. Res. 74 (3) (2003) 393–405.
[13] E. Dorey, et al., Apolipoprotein E, amyloid-beta, and neuroinflammation in Alzheimer's disease, Neurosci. Bull. 30 (2) (2014) 317–330.
[14] X. Li, et al., Clusterin in Alzheimer's disease: a player in the biological behavior of amyloid-beta, Neurosci. Bull. 30 (1) (2014) 162–168.
[15] P. Srivastava, et al., Design and development of some phenyl benzoxazole derivatives as a potent acetylcholinesterase inhibitor with antioxidant property to enhance learning and memory, Eur. J. Med. Chem. 163 (2019) 116–135.
[16] S. Das, S. Basu, Multi-targeting strategies for Alzheimer's disease therapeutics: pros and cons, Curr. Top. Med. Chem. 17 (27) (2017) 3017–3061.
[17] P. Anand, B. Singh, N. Singh, A review on coumarins as acetylcholinesterase inhibitors for Alzheimer's disease, Bioorg. Med. Chem. 20 (3) (2012) 1175–1180.
[18] A.S. Gurjar, et al., In silico studies, synthesis and pharmacological evaluation to explore multi-targeted approach for imidazole analogues as potential cholinesterase inhibitors with neuroprotective role for Alzheimer's disease, Bioorg. Med. Chem. 26 (8) (2018) 1511–1522.
[19] L. Huang, et al., Discovery of indanone derivatives as multi-target-directed ligands against Alzheimer's disease, Eur. J. Med. Chem. 87 (2014) 429–439.
[20] T. Kim, et al., Discovery of benzimidazole derivatives as modulators of mitochondrial function: a potential treatment for Alzheimer's disease, Eur. J. Med. Chem. 125 (2017) 1172–1192.
[21] B. Kuzu, et al., Mono-or di-substituted imidazole derivatives for inhibition of acetylcholine and butyrylcholine esterases, Bioorg. Chem. 86 (2019) 187–196.
[22] Y.S. Lee, et al., Synthesis and structure–activity relationships of tri-substituted thiazoles as RAGE antagonists for the treatment of Alzheimer's disease, Bioorg. Med. Chem. Lett. 22 (24) (2012) 7555–7561.
[23] P. Meena, et al., Synthesis, biological evaluation and molecular docking study of novel piperidine and piperazine derivatives as multi-targeted agents to treat Alzheimer's disease, Bioorg. Med. Chem. 23 (5) (2015) 1135–1148.
[24] H. Irannejad, et al., Synthesis and in vitro evaluation of novel 1, 2, 4-triazine derivatives as neuroprotective agents, Bioorg. Med. Chem. 18 (12) (2010) 4224–4230.
[25] T.T. Kucukkilinc, et al., Synthesis and neuroprotective activity of novel 1, 2, 4-triazine derivatives with ethyl acetate moiety against H 2 O 2 and Aβ-induced neurotoxicity, Med. Chem. Res. 26 (11) (2017) 3057–3071.
[26] A.K. Sen Gupta, et al., Synthesis and evaluation of AChE inhibitory activity of 5, 6-diaryl-1, 2, 4-triazinyloxyacetyl-4-substituted thiosemicarbazides, triazoles and N-benzylidene derivatives, J. Heterocycl. Chem. 20 (3) (1983) 507–510.
[27] M. Yazdani, et al., Multi-target inhibitors against Alzheimer disease derived from 3-hydrazinyl 1, 2, 4-triazine scaffold containing pendant phenoxy methyl-1, 2, 3-triazole: design, synthesis and biological evaluation, Bioorg. Chem. 84 (2019) 363–371.
[28] A. Sinha, et al., Neuroprotective role of novel triazine derivatives by activating Wnt/β catenin signaling pathway in rodent models of Alzheimer's disease, Mol. Neurobiol. 52 (1) (2015) 638–652.
[29] M. Shidore, et al., Benzylpiperidine-linked diarylthiazoles as potential anti-Alzheimer's agents: synthesis and biological evaluation, J. Med. Chem. 59 (12) (2016) 5823–5846.
[30] V. Hepnarova, et al., The concept of hybrid molecules of tacrine and benzyl quinolone carboxylic acid (BQCA) as multifunctional agents for Alzheimer's disease, Eur. J. Med. Chem. 150 (2018) 292–306.
[31] J. Korabecny, et al., 7-MEOTA–donepezil like compounds as cholinesterase inhibitors: Synthesis, pharmacological evaluation, molecular modeling and QSAR studies, Eur. J. Med. Chem. 82 (2014) 426–438.
[32] A. Abou, F. Foubelo, M. Yus, Selective Lithiation of 1-Chloro-n-Phenylsulfanylalkanes, Michigan Publishing, University of Michigan Library, Ann Arbor, MI, 2006.
[33] J.N. Sangshetti, et al., Ceric ammonium nitrate catalysed three component one-pot efficient synthesis of 2, 4, 5-triaryl-1H-imidazoles, J. Chem. Sci. 120 (5) (2008) 463–467.
[34] L.B. Rubia, R. Gomez, TLC sensitivity of six modifications of Dragendorff's reagent, J. Pharm. Sci. 66 (11) (1977) 1656–1657.
[35] M. Recanatini, A. Cavalli, C. Hansch, A comparative QSAR analysis of acetylcholinesterase inhibitors currently studied for the treatment of Alzheimer's disease, Chem. Biol. Interact. 105 (3) (1997) 199–228.
[36] A. Villalobos, et al., Novel benzisoxazole derivatives as potent and selective inhibitors of acetylcholinesterase, J. Med. Chem. 37 (17) (1994) 2721–2734.
[37] A. Rampa, et al., Acetylcholinesterase inhibitors: synthesis and structure–activity relationships of ω-[N-Methyl-N-(3-alkylcarbamoyloxyphenyl)-methyl] aminoalkoxyheteroaryl derivatives, J. Med. Chem. 41 (21) (1998) 3976–3986.
[38] M. Bajda, et al., Structure-based search for new inhibitors of cholinesterases, Int. J. Mol. Sci. 14 (3) (2013) 5608–5632.
[39] P. Taylor, S. Lappi, Interaction of fluorescence probes with acetylcholinesterase. Site and specificity of propidium binding, Biochemistry 14 (9) (1975) 1989–1997.
[40] N.N. Tavares, A. Hasson-Voloch, Choline Acetyltransferase from the electric organ of Electrophorus electricus (L.)–physicochemical characterization and immunochemical identification, Zeitschrift für Naturforschung C 53 (5–6) (1998) 407–415.
[41] E. Nepovimova, et al., Multitarget drug design strategy: quinone–tacrine hybrids designed to block amyloid-β aggregation and to exert anticholinesterase and antioxidant effects, J. Med. Chem. 57 (20) (2014) 8576–8589.
[42] I. Klinkenberg, A. Blokland, The validity of scopolamine as a pharmacological model for cognitive impairment: a review of animal behavioral studies, Neurosci. Biobehav. Rev. 34 (8) (2010) 1307–1350.
[43] G.L. Ellman, et al., A new and rapid colorimetric determination of acetylcholinesterase activity, Biochem. Pharmacol. 7 (2) (1961) 88–95.
[44] S.K. Shrivastava, et al., Design and development of novel p-aminobenzoic acid derivatives as potential cholinesterase inhibitors for the treatment of Alzheimer's disease, Bioorg. Chem. 82 (2019) 211–223.
[45] A. Wolf, et al., A comprehensive behavioral test battery to assess learning and memory in 129S6/Tg2576 mice, PLoS One 11 (1) (2016) e0147733.
[46] G. Kryger, I. Silman, J.L. Sussman, Structure of acetylcholinesterase complexed with E2020 (Aricept®): implications for the design of new anti-Alzheimer drugs, Structure 7 (3) (1999) 297–307.